

Single tilted Bragg reflector fiber laser for simultaneous sensing of refractive index and temperature

Allan C. L. Wong,^{1,*} W. H. Chung,² Hwa-Yaw Tam,² and Chao Lu¹

¹Photonics Research Centre, Department of Electronic and Information Engineering,
Hong Kong Polytechnic University, Kowloon, Hong Kong

²Photonics Research Centre, Department of Electrical Engineering,
Hong Kong Polytechnic University, Kowloon, Hong Kong

*enallan@polyu.edu.hk

Abstract: A type of fiber laser, called tilted Bragg reflector fiber laser (TBR-FL), is proposed and its application in simultaneous sensing of surrounding refractive index (SRI) and temperature is demonstrated. This FL is formed by a pair of wavelength and tilt-angle matched tilted fiber Bragg gratings (TFBGs) that acted both as a resonant cavity and sensing element. A unique spectral feature of the TBR-FL is the presence of grating tilt-induced cladding modes spectrum that does not appear in other type of FL, which provides an extra sensing mechanism. By employing a simple experimental setup with the discrete wavelet transform as the demodulation technique, simultaneously sensing of SRI and temperature are achieved by measuring and analyzing the wavelet coefficients shifts of the laser output and averaged cladding modes.

©2011 Optical Society of America

OCIS codes: (060.2370) Fiber optics sensors; (060.3510) Lasers, fiber; (060.3735) Fiber bragg gratings; (280.3420) Laser sensors.

References and links

1. O. Frazão, L. A. Ferreira, F. M. Araujo, and J. L. Santos, "Applications of fiber optic grating technology to multi-parameter measurement," *Fiber Integr. Technol.* **24**(3), 227–244 (2005).
2. Y. Zhao, and Y. B. Liao, "Discrimination methods and demodulation techniques for fiber Bragg grating sensors," *Opt. Lasers Eng.* **41**(1), 1–18 (2004).
3. J. Jung, H. Nam, J. H. Lee, N. Park, and B. Lee, "Simultaneous measurement of strain and temperature by use of a single-fiber Bragg grating and an erbium-doped fiber amplifier," *Appl. Opt.* **38**(13), 2749–2751 (1999).
4. J. Jung, N. Park, and B. Lee, "Simultaneous measurement of strain and temperature by use of a single fiber Bragg grating written in an erbium:ytterbium-doped fiber," *Appl. Opt.* **39**(7), 1118–1120 (2000).
5. X. Shu, B. A. L. Gwandu, Y. Liu, L. Zhang, and I. Bennion, "Sampled fiber Bragg grating for simultaneous refractive-index and temperature measurement," *Opt. Lett.* **26**(11), 774–776 (2001).
6. T. V. Djambova, and T. Mizunami, "Simultaneous sensing of temperature and displacement using a multimode fiber Bragg grating," *Jpn. J. Appl. Phys.* **39**(Part 1, No. 3B), 1566–1570 (2000).
7. C. L. Zhao, X. Yang, M. S. Demokan, and W. Jin, "Simultaneous temperature and refractive index measurements using a 3° slanted multimode fiber Bragg grating," *J. Lightwave Technol.* **24**(2), 879–883 (2006).
8. Y. Miao, B. Liu, and Q. Zhao, "Simultaneous measurement of strain and temperature using single tilted fiber Bragg grating," *Electron. Lett.* **44**(21), 1242 (2008).
9. Y. G. Han, T. V. A. Tran, S. H. Kim, and S. B. Lee, "Multiwavelength Raman-fiber-laser-based long-distance remote sensor for simultaneous measurement of strain and temperature," *Opt. Lett.* **30**(11), 1282–1284 (2005).
10. T. V. A. Tran, Y. G. Han, S. H. Kim, and S. B. Lee, "Long-distance simultaneous measurement of strain and temperature based on a fiber Raman laser with a single fiber Bragg grating embedded on a quartz plate," *Opt. Lett.* **30**(13), 1632–1634 (2005).
11. O. Hadeler, E. Rønnekleiv, M. Ibsen, and R. I. Laming, "Polarimetric distributed feedback fiber laser sensor for simultaneous strain and temperature measurements," *Appl. Opt.* **38**(10), 1953–1958 (1999).
12. O. Hadeler, M. Ibsen, and M. N. Zervas, "Distributed-feedback fiber laser sensor for simultaneous strain and temperature measurements operating in the radio-frequency domain," *Appl. Opt.* **40**(19), 3169–3175 (2001).
13. P. Childs, A. C. L. Wong, I. Leung, G. D. Peng, and Y. B. Liao, "An in-line in-fibre ring cavity sensor for localized multi-parameter sensing," *Meas. Sci. Technol.* **19**(6), 065302 (2008).
14. A. C. L. Wong, P. A. Childs, and G. D. Peng, "Simultaneous demodulation technique for a multiplexed fiber Fizeau interferometer and fiber Bragg grating sensor system," *Opt. Lett.* **31**(1), 23–25 (2006).

15. A. C. L. Wong, P. A. Childs, and G. D. Peng, "Multiplexed fibre Fizeau interferometer and fibre Bragg grating sensor system for simultaneous measurement of quasi-static strain and temperature using discrete wavelet transform," *Meas. Sci. Technol.* **17**(2), 384–392 (2006).
 16. Y. Miao, B. Liu, S. Tian, and Q. Zhao, "Temperature-insensitive refractive index sensor based on tilted fiber Bragg grating," *Microw. Opt. Technol. Lett.* **51**(2), 479–483 (2009).
 17. C. F. Chan, C. Chen, A. Jafari, A. Laronche, D. J. Thomson, and J. Albert, "Optical fiber refractometer using narrowband cladding-mode resonance shifts," *Appl. Opt.* **46**(7), 1142–1149 (2007).
-

1. Introduction

Up to present, there are mainly two types of grating based fiber lasers (FLs), namely distributed feedback and distributed Bragg reflector FLs, and enormous amount of efforts have been put into the study of their fundamental properties and applications, including fiber sensing. When used as sensing elements, FLs, as active sensors, have the advantage of high sensitivity, sensing output power and extinction ratio, and narrower linewidth/bandwidth. Furthermore, simultaneous two-parameter sensing, especially using only one single sensing element, has attracted considerable research interests. This is driven by: (i) the capability of detecting more measurands using fewer sensors; and (ii) the ability of solving the issue of cross-sensitivity (mostly temperature-induced) inherited from the sensor property [1,2]. Additionally, single sensor has the advantage that its structure can be made more compact, and is generally less difficult to fabricate, which simplifies and eases the packaging and installation works for practical applications.

Thus far, most of the proposed single sensors for simultaneous two-parameter sensing are of passive type [3–8] and only very few on using active sensors, e.g., fiber Raman lasers [9,10] and distributed feedback FLs [11,12] for simultaneous sensing of strain and temperature. Here, we propose a type of grating based FL called the tilted Bragg reflector fiber laser (TBR-FL), and demonstrate its application in simultaneous two-parameter sensing. The TBR-FL comprises a pair of wavelength and tilt-angle matched tilted fiber Bragg gratings (TFBGs), and possesses a unique spectral feature that does not appear in any other type of FLs – the presence of grating tilt-induced cladding modes spectrum. This provides an extra sensing mechanism for the FL to be capable of detecting the surrounding environment. We demonstrate that, with a simple experimental setup, the use of a single TBR-FL for simultaneous sensing of surrounding refractive index (SRI) and temperature. The discrete wavelet transform (DWT) technique is employed to demodulate, denoise and analyze the sensor signal.

2. Fiber laser sensing principle and fabrication

The structure of the TBR-FL comprises a pair of wavelength and tilt-angle matched TFBGs forming the resonant cavity and is depicted in Fig. 1(a). When a pump source is launched, optical feedback inside the cavity confined by the grating pair caused light to amplify, as for the case of ordinary FLs. Lasing occurs at the Bragg mode bound inside the core, whereas the cladding modes are coupled out from the core and so do not contribute to the laser operation. However, these cladding modes have a well-known property that the transmission loss dips vary upon changes in the surrounding refractive index (SRI), while the bound core (lasing) mode remains unaltered. That is, the SRI only affects the cladding modes spectrum and the lasing mode (and hence, lasing wavelength) is kept unchanged. On the other hand, temperature change affects the FL as a whole and alters the entire spectrum (including lasing and cladding modes). Thus, by combining these two sensing properties, simultaneous sensing of SRI and temperature using a single TBR-FL can be achieved, i.e., temperature is measured by tracking the lasing mode shift, and SRI by the differential wavelength shift between the laser output and cladding modes.

The TBR-FL was fabricated in a standard FBG writing facility using the phase mask UV exposure method. First, a high-reflector TFBG was written in a section of stripped erbium-doped fiber (EDF) (Corning Er 1500C) placed immediately behind a phase mask (BRAGG Photonics) by an ArF excimer laser operated at 193 nm (Coherent Compex Pro F2). The TFBG has a tilt angle, grating length and Bragg mode transmission loss of 4.5°, 12.5 mm and

-28.6 dB, respectively, and the spectrum is shown in Fig. 1(b). All spectra were obtained by an optical spectrum analyzer (OSA) (Yokogawa AQ6370, wavelength resolution and sampling interval set to 0.02 nm and 0.001 nm). Next, the UV beam was shifted and an output-coupler TFBG was written with the same tilt angle and grating length as the high-reflector grating. The separation between the closer edges of the two TFBGs, i.e., the nominal cavity, was 1.5 mm. Thus, the FL has a total length of 26.5 mm. Figure 1(c) shows the output spectrum of the TBR-FL, with the lasing wavelength, output power and extinction ratio of 1554.62 nm, -15 dBm and 58 dB, respectively.

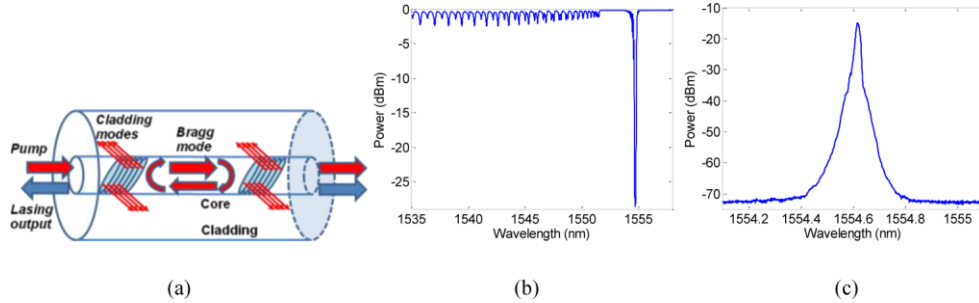


Fig. 1. (a) Structure of the TBR-FL, (b) transmission spectrum of the high reflector grating, and (c) output spectrum of the TBR-FL.

3. Experimental setup and signal demodulation

In order to perform simultaneous sensing of SRI and temperature using a single TBR-FL, it is necessary to get access to both the laser output (Bragg mode) and cladding modes simultaneously. This is done by employing a simple experimental setup as shown schematically in Fig. 2. In this setup, a 980/1550 nm wavelength-division-multiplexer (WDM), and the laser output signal was obtained by the OSA. An optical isolator (ISO) (Lightem) was inserted in between the WDM and OSA to avoid back reflections. At the other side of the FL was a continuous piece of EDF (~50 cm) looped in a diameter of ~3 cm, and so the sensor head comprised both the FL and the short coiled EDF section. Index matching gel (IMG) (Fiber Instruments Sales) was applied to the far end of the EDF to minimize any reflections that may cause resonant feedback. This EDF section acted as an amplified spontaneous emission source (with backward EDF spectrum) when excited by the excessive pump source. As such, the transmission spectrum of the constituent TFBGs can be observed by the OSA. With this setup, both the laser output and cladding modes spectra can be obtained simultaneously. Figure 3(a) shows a typical full spectrum of the TBR-FL, consisting both the laser output [Fig. 3(b)] and cladding modes [Fig. 3(c)] spectra. It should be pointed out that the broad cladding modes spectrum may contain high-frequency AC components due to the Fabry-Perot interference induced by the TFBG pair [13]. However, as will be explained later, these AC components can be readily and automatically removed by the DWT technique without altering the important spectral features.



Fig. 2. Experimental setup.

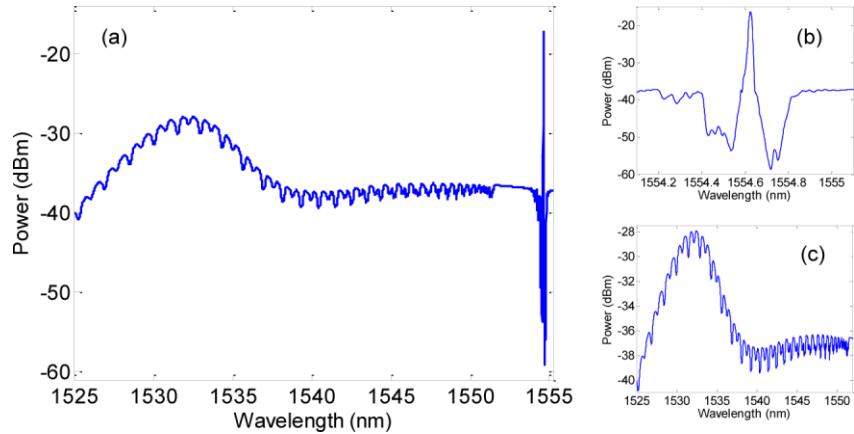


Fig. 3. (a) Full spectrum of the TBR-FL sensor; and the magnification around (b) the laser output and (c) cladding modes spectrum.

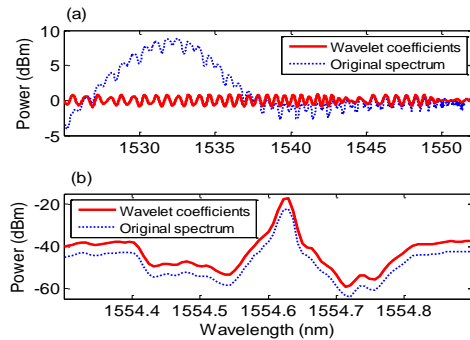


Fig. 4. Wavelet coefficients of a measured TBR-FL transmission spectrum: (a) 6th-level detail coefficients for the cladding modes, and (b) 2nd-level approximation coefficients for the Bragg mode. Dotted lines are the original spectra (manually offset) for comparison.

The TBR-FL sensor signal [Fig. 3(a)] is demodulated and analyzed using the DWT technique [14,15], in which the laser output and cladding modes parts are simultaneously and unambiguously extracted. When the DWT is applied, the sensor signal is decomposed into different spectral bands and represented as detail (high-frequency part) and approximation (low-frequency part) wavelet coefficients at various wavelet levels. Its principle is based on the multiresolution analysis in which the DWT performs a multi-stage two-channel quadrature mirror filter bank operation. The original sensor signal, after processed by the first-stage filtering, is decomposed into 1st-level detail and approximation coefficients, which are the filter coefficients from the high-pass and low-pass parts of the filter bank, respectively. After that, the 1st-level approximation coefficients are used as an input for the 2nd-stage filtering to extract the 2nd-level detail and approximation coefficients. This multi-stage decomposition process is repeated in cascade using the most recent approximation coefficients as the input to the next stage filtering. It is interesting to note that while the approximation coefficients retain the DC values of the original signal, the detail coefficients are mean-removed. Thus, the first few levels of approximation coefficients may have similar spectral profile to the original signal, but indeed the high-frequency components, mostly consisted of noise, are removed because the corresponding levels of detail coefficients are discarded. Since the laser output (lower frequency) and cladding modes (higher frequency) have different spatial frequencies, they are transformed into, and represented as, approximation and detail wavelet coefficients at two separate levels, respectively. E.g., after taking the DWT of the original sensor signal [Fig. 3(a)], Figs. 4(a) and 4(b) show the 6th-level detail coefficients and the 2nd-level approximation coefficients representing the cladding modes and laser output, respectively. For

comparison, the original signal (dotted curve) is also shown. Note that the wavelet transformed signal is in the same domain as the original signal, and so the wavelet coefficients are real-valued that effectively represent the spectral shifts of the TBR-FL signal (both lasing and cladding modes). In Fig. 4(a), a cluster of mean-removed cladding modes having similar ‘spatial frequency’ is extracted, and taking an average of this cluster of modes to measure a parameter would be more accurate than randomly picking one particular mode, as each individual cladding mode responds differently to the same measurand change [16,17]. In Fig. 4(b), the approximation coefficients preserved major feature of the original laser signal with the noisy components removed.

An advantage of using the DWT technique is the removal of noisy components through a wavelet denoising method called the block-level thresholding that is incorporated with the DWT demodulation [15]. This denoising method is particularly useful in removing white noise that spans across the entire signal spectrum, a type of noise that is difficult to remove using other signal processing or filtering techniques. Thus, noise such as random jitter and TFBG pair induced Fabry-Perot interference can be readily and conveniently removed.

4. Simultaneous temperature and SRI sensing

Having established the signal acquisition and demodulation techniques, we demonstrate an application of TBR-FL in simultaneous sensing of SRI and temperature. First, for temperature sensing, with the experimental setup shown in Fig. 2, the sensor head (consisting both the TBR-FL and coiled EDF part) was placed inside a bath of hot water. Temperature was varied by letting the water to cool naturally and was measured by a digital thermometer (Fluke 52II with K-type thermocouple). The measured range was between 31°C – 71°C taken at intervals of 1°C. By employing the DWT demodulation (as in Fig. 4), the wavelet coefficients shifts of the laser output (2nd-level approximation coefficients) and an average of about 20 cladding modes (all are 6th-level detail coefficients) in response to the temperature change is shown in Fig. 5. Solid lines are the linear regression fits of the data points. From the figure, both the laser output and averaged cladding modes yielded a very similar temperature-induced sensitivity, having the values of 10.75 pm/°C ($R^2 = 0.9991$) and 10.88 pm/°C ($R^2 = 0.9975$), respectively. With such a high degree of correlation, it is sufficient to measure the temperature change by tracking the lasing wavelength shift alone.

Next, for SRI sensing, the TBR-FL (excluding the extended EDF part) was placed inside a container filled with pre-mixed and saturated glucose solution (Dextrosol D-Glucose powder), and the SRI was changed by diluting the solution with water, which ensured the solution was fully soluble and homogeneous to avoid any undesired light scattering. The SRI varied in the range of 1.3334 (water) – 1.4137 (glucose solution) with the temperature varied between 23.8°C – 24.3°C during the experiment, and both were obtained by a digital refractometer (Reichert AR200). Similar to the temperature experiment, after applying the DWT to the measured spectra, Fig. 6 shows the wavelet coefficients shifts of the laser output and averaged cladding modes as a function of the SRI change. It is clear that the laser output remained at the zero value (within measurement errors) and so have no direct relationship with the SRI. Furthermore, from the raw lasing spectra the peak power remained at around –16.2 dBm throughout the SRI measurement. This indicated that the SRI only influenced the cladding modes and not the bound core lasing mode, and so both the lasing wavelength and power were unaffected. The averaged cladding modes varied nonlinearly with SRI, and within the measured range the empirical relationship can be described by a 4th-degree polynomial function, $\Delta\lambda_{cladding}(n) = 358.2n^4 - 1432.1n^3 + 1910.1n^2 - 849.9n$ ($R^2 = 0.9998$). Thus, the SRI change can be obtained from the wavelet coefficients shift of the averaged cladding modes, as the laser output is not sensitive to it.

Having investigated the individual temperature and SRI sensing characteristics, simultaneous sensing of these two measurands using a single TBR-FL can be achieved. Temperature change can be obtained from the wavelet coefficients (i.e., wavelength) shift of the laser output, whereas SRI change from the differential wavelet coefficients shift between

the averaged cladding modes and laser output. That is, the residual amount of the wavelet coefficients shift of the averaged cladding modes after subtracting from that of the laser output. As such, Fig. 6 can be used as a look-up table to find the SRI from the differential wavelet coefficients shift.

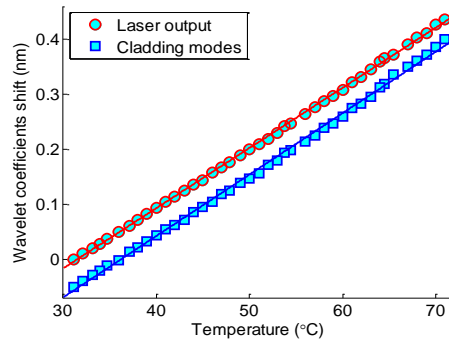


Fig. 5. Wavelet coefficients shift of the laser output and averaged cladding modes as a function of temperature. Lines are the linear regression fits. The cladding modes curve is manually offset by 0.05 nm for ease of viewing.

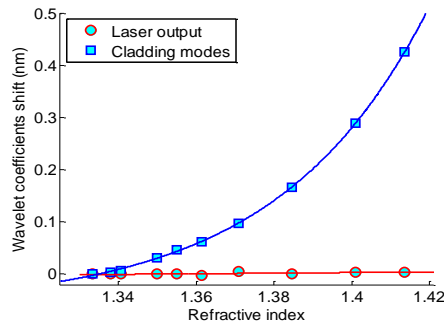


Fig. 6. Wavelet coefficients shift of the laser output and averaged cladding modes as a function of refractive index. Lines are the linear and 4th-degree polynomial regression fits, respectively.

5. Conclusion

A type of FL called TBR-FL has been proposed and fabricated, and an application in the simultaneous sensing of SRI and temperature has been demonstrated. The TBR-FL has a unique feature over other FLs, which is the grating-tilt induced cladding modes spectrum. In response to temperature change, both the lasing and cladding modes correlated very well with each other. For SRI measurement, while the laser output was unaffected, the cladding modes varied nonlinearly, with the relationship best described by a 4th-degree polynomial function. Simultaneous sensing of SRI and temperature was achieved from the fact that the SRI change can be obtained by the differential wavelet coefficients shift between the laser output and cladding modes, and the temperature change by the lasing wavelength shift alone.

Acknowledgments

This work was supported by the Hong Kong Polytechnic University Central Research Grant (grant no. G-YX2C). The authors thank H. J. Wang and D. Chen for their assistance in the fiber laser fabrication.